

High Accuracy Imaging Polarimetry with NICMOS¹

D. Batcheldor,² G. Schneider,³ D. C. Hines,⁴ G. D. Schmidt,³ D. J. Axon,⁵ A. Robinson,⁵ W. Sparks⁶ & C. Tadhunter⁷

Abstract. The ability of NICMOS to perform high accuracy polarimetry is currently hampered by an uncalibrated residual instrumental polarization at a level of 1.2–1.5%. To better quantify and characterize this residual we obtained observations of three polarimetric standard stars at three separate space-craft roll angles. Combined with archival data, these observations were used to characterize the residual instrumental polarization to enable NICMOS to reach its full polarimetric potential. Using these data, we calculate values of the parallel transmission coefficients that reproduce the ground-based results for the polarimetric standards. The uncertainties associated with the parallel transmission coefficients, a result of the photometric repeatability of the observations, dominate the accuracy of p and θ . However, the new coefficients now enable imaging polarimetry of targets with $p \approx 1.0\%$ at an accuracy of $\pm 0.6\%$ and $\pm 15^\circ$.

1. Introduction

The Near Infrared Camera and Multi-Object Spectrometer (NICMOS) is the *only* near infrared (NIR) instrument capable of the high resolution, high fidelity polarimetry needed to examine the scattering geometry and materials in many types of astronomical objects. However, there have been recent reports of a systematic residual instrumental polarization of $\sim 1.5\%$ (Ueta, Murakawa & Meixner 2005) that would seriously compromise studies of objects such as active galactic nuclei and regions within circumstellar protoplanetary disks; they typically exhibit polarizations of $< 5\%$. A comprehensive study of this residual polarization was carried out by Batcheldor et al. (2006, B06), who found a residual excess polarization of $\approx 1.2\%$ in the NIC2 camera.

¹Based on observations made with the NASA/ESA Hubble Space Telescope obtained at the Space Telescope Science Institute, which is operated by the Association of Universities for Research in Astronomy, Incorporated, under NASA contract NAS 5-26555.

²Center for Imaging Science, Rochester Institute of Technology, 54 Lomb Memorial Drive, Rochester, NY, 14623, USA

³Steward Observatory, The University of Arizona, 933 N. Cherry Avenue, Tucson, AZ, 85721, USA

⁴Space Science Institute, 4750 Walnut Street, Suite 205, Boulder, CO 80301, USA

⁵Department of Physics, Rochester Institute of Technology, 54 Lomb Memorial Drive, Rochester, NY, 14623, USA

⁶Space Telescope Science Institute, 3700 San Martin Drive, Baltimore, MD, 21218, USA

⁷Department of Physics & Astronomy, University of Sheffield, Sheffield, S3 7RH, UK

Table 1. Details of Polarimetric Standards

Target	Type	m_v	m_j	m_k	0.55 μm	2.00 μm ($p\%$, θ)	2.04 μm
VR 84c (WKK F7)	B5V	10.3	9.34	9.13	5.98,118°	1.25,126°	1.19,126°
VSS VIII-13	K1III	12.7	9.65	8.68	2.25,102°	0.91,102°	0.86,102°
HD 331891	A4III	9.3	8.80	8.72	0.04,n/a

Prior to this work, observations of only one polarized and one unpolarized standard have been made, each at only two celestial orientation angles. Therefore, until now, it has been impossible to entirely characterize the NICMOS residual polarization. Polarization measurements at three well separated roll angles are necessary to remove the dependence of the measured Stokes parameters on the relative transmission of each of the filters. We report here the findings of a calibration program that collected such data.

2. Observations and Data Reduction

The observations addressed the NICMOS residual polarization and several other key issues, including possible dependence with detector quadrants, source color dependence, the inter-pixel response functions (IPRFs) and latent image persistence. All orbits were scheduled so not to be impacted by the effects of the South Atlantic Anomaly. Persistence can be mitigated with an effective image dithering strategy. However, a precise dithering pattern has to be chosen to avoid image raster overlaps of the PSF diffraction spikes. The observations were dithered in each detector quadrant to circumvent the effects of the IPRFs and sample around defective pixels. The pointing offsets covered a phase spacing of $-1/3$, 0 and $+1/3$ pixels to best tile the IPRFs for the dither pattern employed. The dither steps were sufficiently large so that the 2nd Airy PSF maxima from each dither (0'58, 7.6 pixels), did not overlap from position to position.

The three polarimetric standard stars presented in Table 1 were observed at three separate space craft roll angles. This provides the data for a unique determination of any residual instrumental polarization relative to the equatorial reference frame. The technique allows the polarimetric analysis, derived from the three polarizers at each of the field orientations, to be decoupled and checked for consistency. For comparison with the NIC2 data, the ground-based polarization measurements are corrected to 2.00 μm using the known wavelength dependence of interstellar polarization (Serkowski, Mathewson & Ford 1975).

It is essential to inspect the fidelity of each pointed observation. Instrumental sources of variation in the photometry, not directly resulting from the intrinsic polarization of the target, must be mitigated. Therefore, radially increasing aperture photometry was performed at each pointing and the encircled count rates extracted. Radial profiles that showed more than a 2σ deviation from the average profile were removed from further study.

The determination of p and the orientation of polarization (θ) is addressed for NICMOS by Hines, Schmidt & Schneider (2000, HSS) and B06. In order

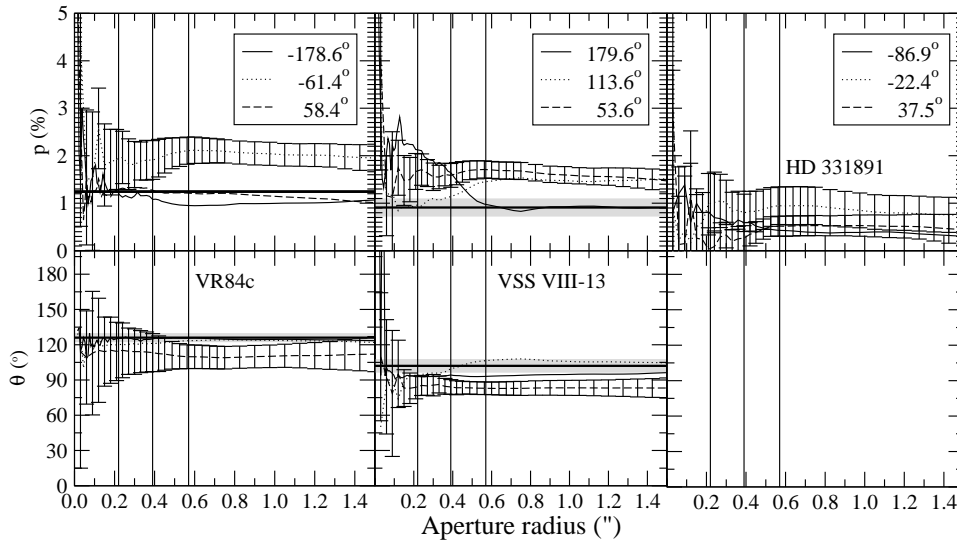


Figure 1. The results using the previous calibration. The thick solid lines show the ground based results and the grey shaded areas show the uncertainties associated with those ground-based results. Error bars are only shown for the cases where they do not overlap the ground based results. The vertical solid lines mark the radii of the 1st, 2nd and 3rd dark minima of the PSF. Each line marks the three celestial field orientations for each target indicated.

to assess the previous polarimetric accuracy, we have applied the coefficients derived by HSS to the new NIC2 calibration data. The results are presented in Figure 1, which demonstrates that at only a few roll angles does the previous calibration reproduce the ground-based results.

3. The Calibration

Since we have observed each standard at multiple space craft roll angles, the uncertainties due to the relative filter transmissions can be removed; each of the three polarizers, separately, was used to collect all the necessary polarimetric data. With these unknowns nullified by the multiple orientations, the only remaining explanation for these residuals (beyond intrinsically smaller uncertainties in the ground-based calibration) is an instrumental polarization (p_i). As p_i is fixed to the space-craft $(Q, U)_i$ are in the instrumental frame; p_i must be determined in Stokes space. Therefore, we determine the actual values and uncertainties of Q and U $(Q, U)_{ac}$, given the ground-based results, and determine $(Q, U)_i$ assuming $(Q, U)_i = (Q, U)_{ob} - (Q, U)_{ac}$. Using this method we find the average instrumental polarization is $0.6 \pm 0.1\%$ at $116 \pm 15^\circ$.

With p_i determined (and subtracted), the parallel transmission coefficients (t_k) that reproduce the ground-based results can then be determined numerically. The parallel transmission for POL240L (t_{240}) is held at 0.9667 as per HSS. B06 also performed this process on archival data, so we include the values of t_k derived by those authors. Table 2 presents the newly derived polarimetric coefficients from this study. There are 13 independent determinations of the

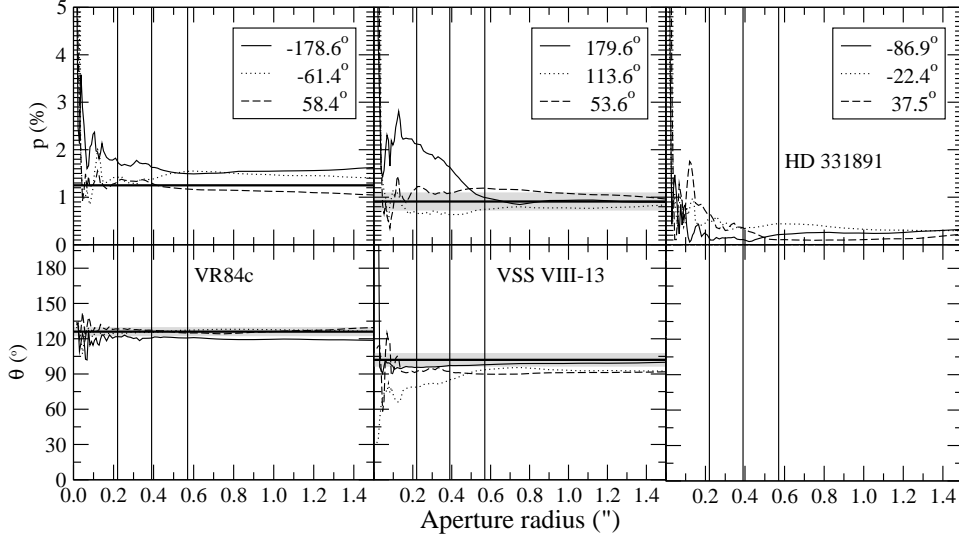


Figure 2. The results from the new calibration. The same convention is used in Figure 1. All results are now consistent with the ground-based data.

Table 2. The New Polarimetric coefficients

Polarizer	ϕ_k (°)	η_k	l_k	t_k
POL0L	8.84	0.7313	0.1552	0.882 ± 0.008
POL120L	131.42	0.6288	0.2279	0.837 ± 0.004
POL240L	248.18	0.8738	0.0673	0.9667

coefficients from each orbit (nine new, four archival), the standard deviation of which is used to define the uncertainty in the coefficients about the mean. These uncertainties are propagated through the calculation of p and θ . As a check, the new coefficients have been applied to the calibration data and presented in Figure 2. This calibration gives results consistent with the ground-based data.

4. Discussions

There are many potential (known and conjectured) sources for the estimated errors on p and θ . However, the uncertainties in the derived transmission coefficients dominate the statistical uncertainties from the photometry. Could these uncertainties be responsible for the observed instrumental polarization? A more accurate way to determine p_i requires observations of an unpolarized flux standard across the whole detector focal plane; this would map the two-dimensional relative transmission differences of the single polarizers. If there is a relative transmission across the focal plane, then this could mimic an instrumental polarization. Therefore, it is appropriate to present the 0.6% value as an instrumental upper limit; p_i could be zero.

When compared with the previous calibration, it can be seen that t_{120} is consistent; t_0 has been changed by 0.5%. Therefore, applying the new values back to previous studies of targets with $p > 5\%$ will not significantly alter the results. However, when applied to targets with $p < 5\%$, the new value of t_{120} results in a very significant improvement in polarimetric accuracy.

We recommend specific observing and data analysis strategies for spatially unresolved, and resolved, targets. For a spatially resolved target (without a bright point source) observers should bin their data to 3×3 pixels (the diffraction limit of the instrument). Dithering can be used to increase spatial resolution and sample around bad pixels. However, high signal to noise ratio data is still critical in determining p and θ to high accuracy. The case of a spatially unresolved source is more complicated. Due to uncorrectable bad pixels, the dithered data must be inspected to identify deviant profiles. This must be done by executing a large number of pointed dithers (with a step size greater than the PSF to avoid persistence). Encircled energy profiles should be derived independently from each observation. A sigma clip should then be used to determine whether an individual profile is deviant or not. The greater number of dithers used, the more accurate the flagging of deviant profiles will be. For small numbers of dither points (not optimally recommended) medianing can be used to coarsely reject outliers. Outside an aperture of radius $0''.57$, the PSF affects disappear. Inside this radius, the uncertainties in p and θ rise rapidly. Observers must weigh the required polarimetric accuracy to the required resolution.

5. Conclusions

Using the multi-roll technique, we have placed an upper limit to the NIC2 instrumental polarization of 0.6%. The instrumental polarization has been subtracted from the target data in the Q, U plane. New parallel transmission coefficients were then derived by forcing p and θ to the same values of the calibration standards. The new coefficients are such a minor change from the previous that it does not warrant the re-analysis of previous NIC2 imaging polarimetry data of highly polarized ($p > 5\%$) targets. Importantly, this improved calibration opens a new domain for observational investigations with *HST* by enabling very high precision polarimetry of intrinsically low ($p < 5\%$) polarization sources.

Acknowledgments. Support for Proposal number HST-GO-10839.01-A was provided by NASA through a grant from the Space Telescope Science Institute, which is operated by the Association of Universities for Research in Astronomy, Incorporated, under NASA contract NAS5-26555.

References

- Batcheldor, D. et al. 2006, PASP, 118, 642
- Hines, D. C., Schmidt, G. D. & Schneider, G. 2000, PASP, 112, 983
- Serkowski, K., Mathewson, D. L., & Ford, V. L. 1975, ApJ, 196, 261
- Turnshek, D. A., Bohlin, R. C., Williamson II, R. L., Lupie, O. L., Koornneef, J., & Morgan, D. H. 1990, AJ, 99, 1243
- Ueta, T., Murakawa, K., & Meixner, M. 2005, AJ, 129, 1625
- Whittet, D. C. B., Martin, P. G., Hough, J. H., Rouse, M. F., Bailey, J. A., & Axon, D. J. 1992, ApJ, 386, 562